

See discussions, stats, and author profiles for this publication at: <https://www.researchgate.net/publication/294091446>

Intracavity-pumped, cascaded AgGaSe 2 optical parametric oscillator tunable from 5.8 to 18 μm

ARTICLE *in* OPTICS EXPRESS · DECEMBER 2015

Impact Factor: 3.49 · DOI: 10.1364/OE.23.033460

READS

40

7 AUTHORS, INCLUDING:



Georgi Marchev

49 PUBLICATIONS 288 CITATIONS

SEE PROFILE



Dmitry Kolker

Novosibirsk State Technical University

36 PUBLICATIONS 145 CITATIONS

SEE PROFILE



Andrius Zukauskas

KTH Royal Institute of Technology

38 PUBLICATIONS 90 CITATIONS

SEE PROFILE



Nadezhda Kostyukova

Novosibirsk State Technical University

14 PUBLICATIONS 4 CITATIONS

SEE PROFILE

Intracavity-pumped, cascaded AgGaSe₂ optical parametric oscillator tunable from 5.8 to 18 μm

Andrey A. Boyko,^{1,2,3} Georgi M. Marchev,¹ Valentin Petrov,^{1,*} Valdas Pasiskevicius,⁴
Dmitry B. Kolker,³ Andrius Zukauskas,⁴ and Nadezhda Y. Kostyukova^{1,2,3}

¹Max-Born-Institute for Nonlinear Optics and Ultrafast Spectroscopy, 2A Max-Born-Str., D-12489 Berlin, Germany

²Special Technologies, Ltd., 1/3 Zeljonaja gorka Str., 630060 Novosibirsk, Russia

³Novosibirsk State University, 2 Pirogova Str., 630090 Novosibirsk, Russia

⁴Department of Applied Physics, Royal Institute of Technology, 10691 Stockholm, Sweden
petrov@mbi-berlin.de

Abstract: A AgGaSe₂ nonlinear crystal placed in a coupled cavity is intracavity pumped by the ~1.85-μm signal pulses of a 1.064-μm pumped Rb:PPKTP doubly-resonant optical parametric oscillator (OPO) operating at a repetition rate of 100 Hz. Using two samples cut for type-I and II phase-matching, the overall idler tunability of the singly-resonant AgGaSe₂ OPO covers an unprecedented spectral range from 5.8 to ~18 μm in the mid-IR.

©2015 Optical Society of America

OCIS codes: (190.4970) Parametric oscillators and amplifiers; (160.4330) Nonlinear optical materials.

References and links

1. V. Petrov, "Frequency down-conversion of solid-state laser sources to the mid-infrared spectral range using non-oxide nonlinear crystals," *Prog. Quantum Electron.* **42**, 1–106 (2015).
2. A. Zakeł, G. J. Wagner, W. J. Alford, and T. J. Carrig, "High-power, rapidly-tunable dual-band CdSe optical parametric oscillator," in *Advanced Solid-State Photonics*, (ASSP, 2005), pp. 433–437.
3. A. Zakeł, G. J. Wagner, W. J. Alford, and T. J. Carrig, "High-power, rapidly-tunable ZnGeP₂ intracavity optical parametric oscillator," in *Conference on Lasers and Electro-Optics* (OSA, 2005), paper CThY5.
4. L. H. Tan and P. B. Phua, "Generation of watt level mid-infrared wavelengths using intra-cavity ZnGeP₂ OPO within a 2.1 μm Ho:YAG laser," *Proc. SPIE* **7917**, 79170O (2011).
5. D. J. Kane, J. M. Hopkins, M. H. Dunn, P. Schunemann, and D. J. M. Stothard, "Tm:YAP pumped intracavity pulsed OPO based on orientation-patterned gallium arsenide (OP-GaAs)," in *6th EPS-QEOD Europhoton Conference on Solid-State, Fibre and Waveguide Coherent Light Sources*, (2014), paper TuA-T1-O-03.
6. P. B. Phua, K. S. Lai, R. F. Wu, and T. C. Chong, "Coupled tandem optical parametric oscillator (OPO): an OPO within an OPO," *Opt. Lett.* **23**(16), 1262–1264 (1998).
7. R. Wu, K. S. Lai, W.-P. E. Lau, H. F. Wong, Y. L. Lim, K. W. Lim, and L. C. L. Li, "A novel laser integrated with a coupled tandem OPO configuration," in *Conference on Lasers and Electro-Optics* (OSA, 2002), paper CTuD6.
8. D. A. Roberts, "Dispersion equations for nonlinear optical crystals: KDP, AgGaSe₂, and AgGaS₂," *Appl. Opt.* **35**(24), 4677–4688 (1996).
9. A. Harasaki and K. Kato, "New data on the nonlinear optical constant, phase-matching, and optical damage of AgGaS₂," *Jpn. J. Appl. Phys.* **36**(1), 700–703 (1997).

1. Introduction

Cascaded or tandem optical parametric oscillators (OPOs) for down conversion of laser radiation into the mid-IR spectral range using non-oxide nonlinear crystals in the second stage have rarely been realized with intracavity pumping [1]. In addition to the more compact and robust design such schemes profit from the higher (intracavity) pump power for the OPO second stage provided by the signal or idler wave of an oxide crystal based OPO first stage, in turn pumped as a rule at 1.064 μm by a Nd:YAG laser system. Compared to pumping inside the cavity of a ns laser, demonstrated in the past with CdSe or ZnGeP₂ (ZGP) in a gain-switched Cr:ZnSe laser [2,3], or more recently with ZGP in a Q-switched Ho:YAG laser [4] and orientation-patterned GaAs (OPGaAs) in a Q-switched Tm:YAP laser [5], the cascaded OPO approach offers the flexibility of selecting the most suitable pump wavelength for broadband tunability of the second stage based on a specific non-oxide nonlinear crystal [1].

The first such realization at a repetition rate of 5 Hz, with a doubly-resonant OPO (DRO) based on ZGP pumped by the o-beam of a near-degenerate, double pump-pass, type-II KTP DRO resulted in an overall conversion efficiency of 5.2% from 1.064 μm to the mid-IR (combined signal and idler energy near degeneracy at 4.2 μm) [6]. A similar set-up with a near-degenerate ZGP DRO operating at 5 kHz was presented in [7]. These demonstrations were characterized by limited tunability, maximum up to about 8 μm [6] determined by the DRO scheme and the crystal choice. In the present work we investigate a singly-resonant OPO (SRO) based on a AgGaSe₂ (AGSe) crystal intracavity pumped at $\sim 1.85 \mu\text{m}$ by the signal pulses of a Rb:PPKTP DRO. Both the choice of a SRO design and the transparency of the AGSe crystal enable coverage of much broader portions of the mid-IR spectral range. With two AGSe samples cut for type-I and II phase-matching an extremely broad tuning range for the nonresonated idler is achieved, extending from 5.8 to $\sim 18 \mu\text{m}$.

2. Experimental set-up and Rb:PPKTP DRO performance

The Rb:PPKTP crystal employed in the first stage was 12-mm long (x-direction, propagation), 8-mm wide (y-direction) and 5-mm thick (z-direction, poling), see Fig. 1(a). The metal electrode grating used had a period of $\Lambda = 38.5 \mu\text{m}$ and was 8 mm long by 5 mm wide. Thus the useful aperture of this uncoated sample was $\sim 5 \times 5 \text{ mm}^2$. The pump source was a diode-pumped multi longitudinal mode, Q-switched at 100 Hz, Nd:YAG laser / amplifier, Fig. 1(b). A combination of a half-wave plate ($\lambda/2$) and a polarizer served as an attenuator. To improve the spatial beam profile (eliminate diffraction rings producing hot spots) a vacuum diamond pinhole was installed in the focus of an expanding telescope. The pump M^2 parameter measured behind the telescope amounted to ~ 2 . The beam size was then reduced by an additional telescope, Fig. 1(b), to a Gaussian diameter (at e^{-2} intensity level) of 2.9 mm in the horizontal and 3.6 mm in the vertical (along the polarization) directions.

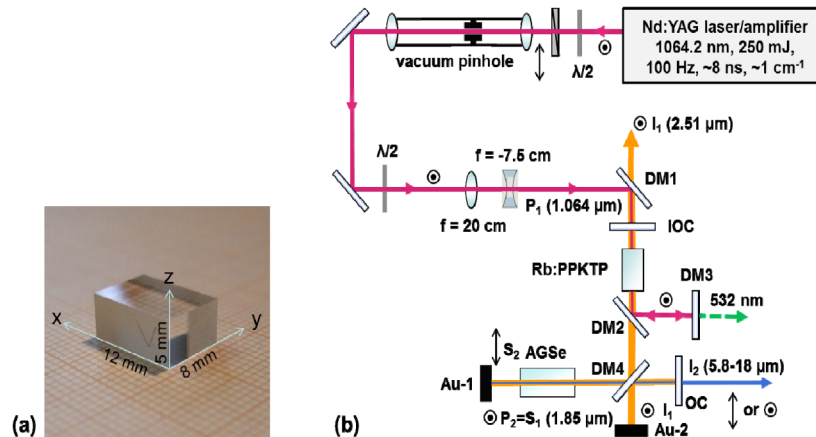


Fig. 1. Photograph of the thick Rb:PPKTP crystal with axis orientation and dimensions (a) and schematic of the intracavity pumped, cascaded AGSe OPO (b).

All mirrors used were plane mirrors. The dichroic mirror DM1 totally reflects the pump (P_1) radiation and highly transmits both signal (S_1) and idler (I_1) from the first stage. The ZnSe input-output coupler (IOC) of the first OPO is highly transmitting for P_1 , highly reflecting for S_1 (96%) but not optimized (transmitting 55%) for I_1 . Thus using a cut-on filter, only the idler, I_1 in Fig. 1(b), from the first stage is monitored at this output. DM2 (Infrasil, clear transparency up to $\sim 3 \mu\text{m}$) is highly reflecting both for the fundamental (1.064 μm) and the second-harmonic of the pump laser and highly transmitting the s-polarized S_1 (96%) and I_1 (91%) waves. DM3 is at 50 mm (physical length) from the IOC and highly reflects P_1 but transmits the second harmonic. Thus a double pump pass in the Rb:PPKTP crystal is realized while the green light parasitically generated in it does not reach the AGSe crystal. The

Rb:PPKTP DRO physical cavity length amounts to ~ 100 mm (arm containing the AGSe crystal) and ~ 90 mm (main idler I_1 beam arm). The physical cavity length of the AGSe SRO is ~ 60 mm. Ideally I_1 will be resonated in the arm containing the Au-2 gold mirror as an end reflector, S_1 - in the arm containing Au-1, and the signal S_2 of the AGSe SRO – between Au-1 and the output coupler (OC). The ZnSe OC is highly reflecting for S_2 only above $2.3 \mu\text{m}$ and transmits $76 \pm 5\%$ in the idler I_2 spectral tuning range up to $15 \mu\text{m}$. This means that this mirror affects the operation of the AGSe SRO at idler wavelengths beyond $9.5 \mu\text{m}$ due to signal outcoupling and beyond $15 \mu\text{m}$ due to idler absorption (transmission is only 43% at $17 \mu\text{m}$). Note that high depletion of the signal S_1 acting as a pump P_2 for the AGSe crystal in the arm containing Au-1, can in principle turn the Rb:PPKTP DRO into a SRO.

Optimum bending dichroic mirror DM4 was not available and two different mirrors were used depending on the I_2 spectral range and the AGSe sample employed. For the AGSe sample #1 which covered the $5.8\text{-}8.3 \mu\text{m}$ I_2 spectral range, a dichroic CaF_2 mirror was used. It totally reflects $S_1 = P_2$ but is not optimized near $2.5 \mu\text{m}$ (I_1 and S_2), where the transmission achieved at 50° angle of incidence is $\sim 70\%$ (both s- and p-polarizations), and for I_2 , for which the transmission is $80 \pm 5\%$ for p-polarization. Thus I_1 is partially resonated also in the arm containing the AGSe crystal while S_2 and I_2 experience some reflection losses. It is impossible to establish whether there is a partial feedback for S_2 from IOC while the reflected by DM4 portion of I_2 is obviously absorbed in the DM2 substrate. For the AGSe sample #2 which covered the $8\text{-}18 \mu\text{m}$ I_2 spectral range, a dichroic ZnSe mirror was used at 45° as DM4. It also totally reflects $S_1 = P_2$ but is not optimized near $2.5 \mu\text{m}$ (I_1), where the transmission for s-polarization is $\sim 50\%$ and for the S_2 tuning range where the transmission for p-polarization is $\sim 75 \pm 5\%$. It transmits $60 \pm 10\%$ in the $8\text{-}15 \mu\text{m}$ idler (I_2) tuning range and absorbs beyond $15 \mu\text{m}$. Thus I_1 is resonated to a similar extent also in the arm containing the AGSe crystal.

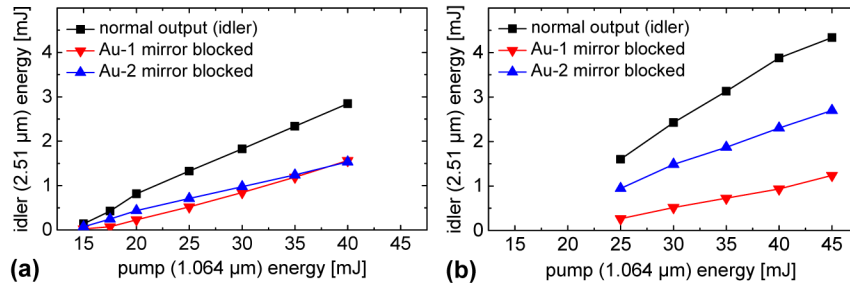


Fig. 2. Performance of the first stage (idler I_1) without the AGSe crystal using different DM4 for the short (a) and long (b) wave mid-IR tuning range of the second stage. The data are corrected for the 91% transmission of DM1.

The performance of the Rb:PPKTP DRO with the entire cavity shown in Fig. 1(b) aligned but with the AGSe crystal removed is shown in Fig. 2. At room temperature the signal S_1 was at $\sim 1.85 \mu\text{m}$ and the idler I_1 - at $\sim 2.51 \mu\text{m}$. The measurable output behind IOC and DM1 consists mainly of the idler and is obviously not optimized for this configuration designed for intracavity pumping of the second stage. Nevertheless, it is seen from the figures that both arms containing the Au-mirrors provide feedback for the idler I_1 . In accordance with the DM4 characteristics, the contribution of the cavity arm containing Au-2 is weaker in the long wave mid-IR (I_2) configuration, Fig. 2(b), compared to the short wave one, Fig. 2(a). In the short wave (for I_2) cavity configuration, the maximum I_1 output energy measured (2.85 mJ) leads to an estimate of 7 mJ for the intracavity S_1 energy that will be used for pumping the second AGSe stage, and P_1 ($1.064 \mu\text{m}$) depletion of 30.5%. With an extrapolated threshold of ~ 12 mJ, Fig. 2(a), the total (S_1 and I_1) internal slope efficiency amounts to $\sim 44\%$. In the long wave (for I_2) cavity configuration, the maximum I_1 output energy measured (4.34 mJ) leads to an estimate of 10.7 mJ for the intracavity S_1 energy that will be used for pumping the second AGSe stage, and P_1 ($1.064 \mu\text{m}$) depletion of 41%. With an extrapolated threshold of ~ 17 mJ, Fig. 2(b), the total (S_1 and I_1) internal slope efficiency reaches $\sim 66\%$.

3. Performance of the AGSe SRO at 100 Hz

The AGSe sample #1 employed in the short wave mid-IR cavity configuration was type-I, cut at $\varphi = 45^\circ$ and $\theta = 52^\circ$. It was 14-mm long with an aperture of $4.5 \times 4.5 \text{ mm}^2$, AR-coated for $S_1 = P_2$ (94% transmission) but with high transmission (87%) also for S_2 and I_1 while in the I_2 spectral range the measured transmission was 70%. For long wavelength generation we employed a type-II AGSe sample (#2) cut at $\varphi = 0^\circ$, $\theta = 51.3^\circ$ because this polarization configuration exhibits higher effective nonlinearity d_{eff} . It was 15-mm long with an aperture of $5 \times 6 \text{ mm}^2$ and similarly AR coated. In the I_2 tuning range the measured transmission exceeded 65% up to $12 \mu\text{m}$, dropping further down to 45% at $15 \mu\text{m}$ and only 5% at $18 \mu\text{m}$ due to intrinsic phonon absorption. The idler I_2 was extracted after a double pass through the crystals.

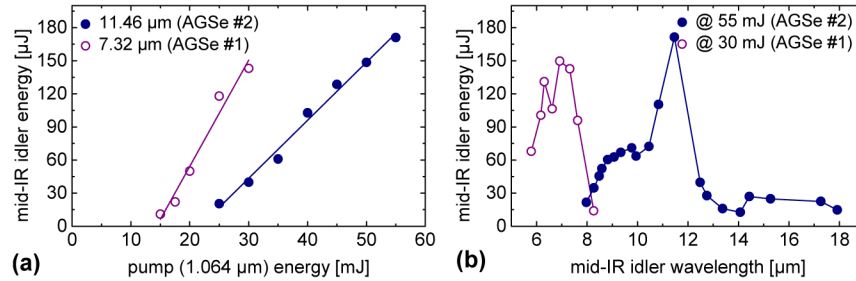


Fig. 3. Idler I_2 energy of the AGSe SRO obtained at normal incidence with the two samples used in dependence on the pump P_1 energy at $1.064 \mu\text{m}$ (a), and angle tuning of the AGSe SRO in the mid-IR at maximum pump levels (b).

Figure 3(a) shows the input-output characteristics of the cascaded OPO for idler I_2 wavelengths of $7.32 \mu\text{m}$ (AGSe sample #1) and $11.46 \mu\text{m}$ (AGSe sample #2) recorded at normal incidence. The maximum output energies obtained ($150 \mu\text{J}$ at $6.92 \mu\text{m}$ and $171 \mu\text{J}$ at $11.46 \mu\text{m}$) are roughly 15 times higher than the energy specified in [6] at the upper wavelength limit of ZGP ($8 \mu\text{m}$). In terms of average power the improvement we have achieved is ~ 300 times. Note that the 5 kHz ZGP DRO described in [7] operated only up to $6 \mu\text{m}$. The angle tuning results for the AGSe SRO are summarized in Fig. 3(b). In both cases it can be seen that at normal incidence there is an enhancement of the OPO feedback. In the case of AGSe #1, d_{eff} remains almost constant in the tuning range, the spectral dependence is affected, however, by the wavelength dependence of the nonlinear coupling, the changing transmission of DM4 for S_2 and the onset of absorption in its substrate for I_2 above $8 \mu\text{m}$. In the case of AGSe #2, d_{eff} increases with the mid-IR idler wavelength. Beyond $9.5 \mu\text{m}$, the performance is affected by the characteristics DM4 for S_2 , beyond $12 \mu\text{m}$ by absorption in the AGSe crystal, and beyond $15 \mu\text{m}$ also by absorption in the DM4 and OC substrates. In addition, the existence of a retracing point in this limit complicates the energy estimation.

The angle tuning data recorded are summarized as symbols in Fig. 4(a). We attempted two fits (shown by lines in the figure) using the most popular Sellmeier equations for AGSe: those from [8] which are specified up to $15.5 \mu\text{m}$ and those from [9], specified up to $16 \mu\text{m}$. It can be seen that in the short wave mid-IR range (AGSe sample #1) the fitting results are similar but in the long wave mid-IR range (AGSe sample #2), the Sellmeier equations of Kato et al. provide a better fit to our results. The largest discrepancy is observed as expected at wavelengths beyond the validity of the equations where the retracing point (two pairs of signal and idler waves) appears. This is shown in Fig. 4(b) where a double peak signal spectrum is presented corresponding to the idler I_2 pair at ~ 14 and $\sim 18 \mu\text{m}$ shown in Fig. 3(b).

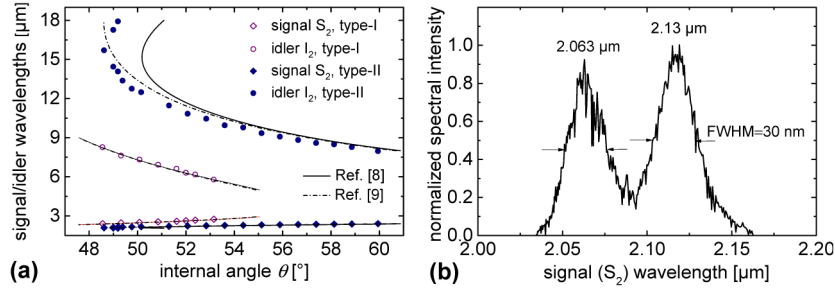


Fig. 4. Angle tuning of the AGSe SRO (a): experimental results (symbols) and fits with Sellmeier expressions from [8] and [9] (lines). High resolution (2 nm) signal spectrum recorded at $\theta = 49.2^\circ$ indicative of retracing behavior (b).

Figure 5(a) shows the spectra of the pump ($P_2 = S_1$) and signal (S_2) pulses of the AGSe SRO. With a low resolution PbS spectrometer, the $P_2 = S_1$ spectrum at $\sim 1.85 \mu\text{m}$ is not well resolved but the FWHM of 23 nm gives an idea about the resolution for the S_2 spectra at $\sim 2.2 \mu\text{m}$ (with AGSe #2) and $\sim 2.5 \mu\text{m}$ (with AGSe #1) measured simultaneously. Independent measurement of the P_1 ($1.064 \mu\text{m}$) spectrum yields a spectral resolution of $\sim 15 \text{ nm}$ for this spectrometer. The correct bandwidth of the $P_2 = S_1$ spectrum was measured by an InGaAs spectrometer yielding a FWHM of 11.5 nm, see Fig. 5(a), which is roughly 2 times narrower than the 25 nm OPO bandwidth acceptance calculated for PPKTP assuming monochromatic pump. This can be explained by spectral narrowing in the Rb:PPKTP OPO. On the other hand, the measured P_2 spectral bandwidth is roughly 3 times larger than the calculated pump spectral acceptance of the AGSe crystal ($\sim 4 \text{ nm}$ both for type-I and type-II). However, such a calculation assumes monochromatic S_2 radiation which is not true for the AGSe SRO where the signal wavelength is not fixed by a spectrally selective element. Thus, this effect is not considered to be a serious limiting factor. Though strictly speaking the FWHM of the S_2 pulses of 28 and 35 nm in Fig. 5(a) is an upper limit, with a spectral resolution of 15 nm it is very close to the actual bandwidth. This is confirmed by the measurement shown in Fig. 4(b) at signal wavelengths still within the sensitivity range of the high resolution InGaAs spectrometer. By convolution of the two spectra (pump and signal) one obtains a spectral bandwidth (FWHM) of $\sim 65 \text{ cm}^{-1}$ (in both cases) for the idler I_2 which translates into 340 nm near $7 \mu\text{m}$ and about 800 nm near $11 \mu\text{m}$.

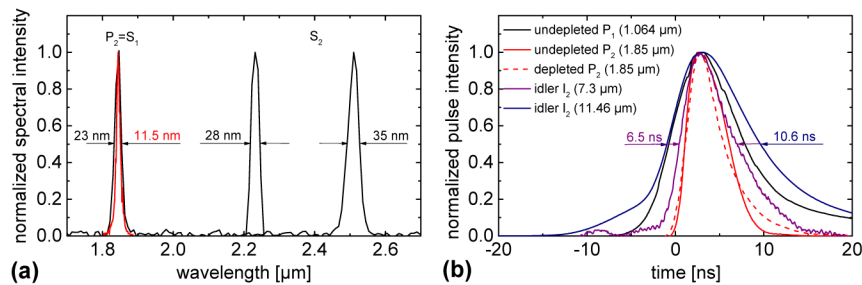


Fig. 5. Low resolution spectra of the $P_2 = S_1$ and S_2 pulses (black lines) at maximum power and high resolution spectrum of the $P_2 = S_1$ pulses (red line) (a). Temporal shapes of the pump laser pulse at $1.064 \mu\text{m}$ (P_1), the $P_2 = S_1$ pulse without the AGSe crystal and with the second stage operating, and the idler I_2 pulse at 7.32 and $11.46 \mu\text{m}$ (b).

Figure 5(b) shows the temporal pulse shapes (arbitrarily normalized to a common maximum) measured for the type-I and type-II AGSe SROs in the near-IR with a 70 ps response InGaAs photodiode, and in the mid-IR - by a (HgCdZn)Te detector with a rise time of 2 ns. Since the last measurement was not corrected for this finite response it can be concluded that all pulses are shorter than the 8-ns long P_1 ($1.064 \mu\text{m}$) pump. In Fig. 5(b) one can also see the depletion of the P_2 pulse when the AGSe SRO is operating.

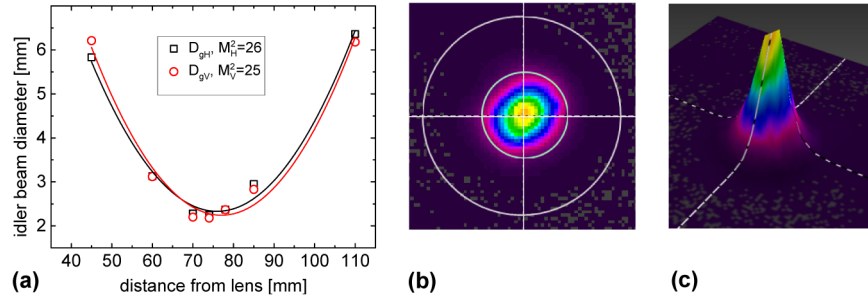


Fig. 6. M^2 measurements of the I_2 idler ($11.46 \mu\text{m}$) and its 2D (b) and 3D (c) beam profile at 70 mm from the $f = 50 \text{ mm}$ BaF_2 lens.

The mid-IR idler beam profiles were recorded for the type-II AGSe crystal at 45 mJ pump energy ($1.064 \mu\text{m}$) by a SpiriconTMPyrocam III camera equipped with a LiTaO_3 pyroelectric detector (active area, $12.4 \text{ mm} \times 12.4 \text{ mm}$; element size, $0.1 \text{ mm} \times 0.1 \text{ mm}$), see Fig. 6. The software automatically evaluates the beam diameters at the $1/e^2$ intensity level. The results of the M^2 fits by Gaussian diameters are shown in Fig. 6(a). The M^2 values in the horizontal plane and vertical (critical) plane were very close but the beam waists were slightly displaced indicating slight astigmatism. Figures 6(b) and (c) show 2D and 3D images of the mid-IR idler beam profile at $11.46 \mu\text{m}$ indicating almost circular shape.

4. Conclusion

In conclusion, we investigated an intracavity-pumped, cascaded AGSe OPO generating idler pulses in the $5.8\text{--}18 \mu\text{m}$ spectral range. The upper limit represents the longest wavelength ever generated with an OPO based on AGSe [1]. The maximum mid-IR pulse energy at 100 Hz reached $171 \mu\text{J}$ at $11.46 \mu\text{m}$. Maximized extraction of this idler I_2 (through optimized mirrors DM4 and OC) alone would increase this level to about $350 \mu\text{J}$.

Further increase of the overall efficiency can be expected by improved characteristics of DM4 at I_1 and S_2 (maximum transmission), extending the S_2 reflectivity of OC to shorter wavelengths and increasing the I_1 reflectivity of IOC. In this case only the depletion in the AGSe crystal will play the role of a loss mechanism for the Rb:PPKTP DRO. This depletion in the present experiment can be estimated to be over 35% leading to an overall internal quantum conversion efficiency of $\sim 8\%$ from the $1.064 \mu\text{m}$ pump pulse or $\sim 4\%$ if the available I_2 output is considered (external conversion efficiency). The estimation is based on the monitored I_1 output behind the IOC mirror. While the insertion of the AGSe crystal does not substantially increase the threshold of the Rb:PPKTP DRO, the slope is drastically reduced and the available $S_1 = P_2$ pulse intracavity energy at maximum pump level is roughly 3 times lower. Improving the above mentioned mirror characteristics is expected to suppress this effect and substantially increase the overall conversion efficiency from the $1.064 \mu\text{m}$ pump to the mid-IR idler pulse.

Power scaling can be achieved increasing the beam sizes and such experiments are also planned for the near future.

Acknowledgments

A.A.B. and N.Y.K. acknowledge mobility support through the DAAD Michail-Lomonosov-Programme - Linie A, 2014 (ID 50015386) and 2015 (ID 57180771), respectively. We also acknowledge partial financial support from the Ministry of Education and Science of the Russian Federation, Project # RFMEFI57814X0042 and from the Swedish Research Council, Grant # 621-2012-2430.